

# NovAtel's RT-20 -- A Real Time Floating Ambiguity Positioning System

Tom J. Ford and Janet Neumann

NovAtel Communications Ltd  
6732 8 Street N.E.  
Calgary, Alberta, Canada T2E 8M4  
1994

## BIOGRAPHY

Tom Ford graduated from the University of Waterloo in 1975 with a B.Math and from the University of Toronto in 1981 with a B.Sc. Until 1989 he designed and implemented software for inertial, doppler and GPS survey systems for Nortech Surveys Ltd. Since then he has been an integral part of the signal processing and navigation team at NovAtel communications where he is a GPS specialist.

Janet Neumann received her BS in Electrical Engineering in 1978 and her MS in Electrical Engineering in 1981 from the University of Kansas and Iowa State University, respectively. Since 1983, she has been involved in many aspects of GPS algorithm design and implementation. Her focus for the last three years has been on signal analysis and carrier phase positioning algorithms.

## ABSTRACT

Over the past 10 years, the thrust of many GPS programs has been towards solving the precise positioning problem with a fixed integer carrier solution. Progress has been made in this area, but an uncertain multipath environment and decorrelated ionospheric delays have made this technology problematic for a single frequency receiver. The nature of the solution requires an excess of computing resources and a lot of time, if special initialization methods are not used. NovAtel has developed a high performance floating ambiguity differential positioning package on a single board which promises to be as robust as a differential pseudorange system but approaches the accuracy achievable with a fixed ambiguity single frequency system. The process is described in this paper, including its features, data stream, positioning filters and test methods and results.

## INTRODUCTION

In 1992 NovAtel began a program to implement a double difference positioning algorithm based on the carrier phase measurements from its GPSCard 2151R, a Narrow Correlator, C/A code receiver that tracks the L1 GPS frequency. The goal was to develop ambiguity fixing technology which could be used in a variety of applications. By September of 1993 we had a real time L1 ambiguity fixing routine which ran successfully on a 486 PC with a resident GPSCard. However, there were some significant problems involved in making the transition from an engineering development system to a product for the commercial market.

The first problem involved the mechanics of the searching process. Since a reliable search for ambiguities on single frequency data entails searching many different ambiguity combinations, the RAM and throughput requirements were too *extensive* to allow its implementation on our current receiver board. This meant additional cost plus the awkwardness of extra hardware for the customer. It also meant that the customer either had to get data from two sources (the PC and the GPSCard) or we had to do some extensive data rerouting which would be costly in throughput and development time.

The next problem was based on the fact that there is an inherent tradeoff in real-time integer fixing between time-to-decision, and the reliability of that decision. This tradeoff doesn't exist with a post-processing system. In that case, one simply looks at all the data, then makes the best decision possible. If the real-time system is optimized for a quick decision, then there will be cases (dependent on multipath or ionospheric activity) where it makes a wrong decision. But to be always reliable, it must take much longer than it normally needs to make its decision, because the time and certainty needed to make a decision varies greatly depending on the multipath and atmospheric effects. Since we would be selling to a great

variety of users, in a great variety of multipath and atmospheric environments. It was hard to know how to set the decision criterion. Some users might want it optimized for decision speed. These would be people who worked in benign atmospheric and multipath environments could handle an occasional error, and would be knowledgeable enough to recognize the symptoms of an incorrect ambiguity choice. Others might want a system which virtually guaranteed a correct decision. Most would want their own decision to point somewhere in between. There were two choices: a) pick a decision criterion which tried to suit everyone, but which actually suited no one well, or b) design a system with user input, attempting to accommodate everyone, but which would be difficult to use.

Confronted with these problems, we decided to delay the implementation of the real-time integer fixing system until our NovAtel L1L2 boards were available and instead find an interim solution to the positioning problem which could increase the performance of our existing technology until the next generation of receivers became available.

The floating ambiguity positioning algorithm was a subset of the fixed ambiguity search routines. It was used to initially define the limits of the search space, and ran in parallel with the fixed solution once the ambiguities had been resolved. We found that the floating and fixed ambiguity solutions agreed very well and that the floating solution was more stable than the fixed solution. In addition, the floating routines worked more efficiently in kinematic mode because a large number of filters representing the wrong ambiguities didn't have to be maintained. Finally, the floating solution routines required some 10% of the memory allocated for the fixed ambiguity process and had a more balanced processing load.

Based on the strengths we saw during this experience, we decided to integrate the floating ambiguity filter with the twelve channel MINOS2 generation of receivers. This would provide a product that was as stable as a pseudorange differential solution but that would be almost an order of magnitude more accurate. The integration included the development of an efficient data packet carrying both phase and pseudorange data, additional logic to improve the kinematic estimation of ambiguities and a new method to eliminate the effect of the transmission latency of the differential data.

NovAtel now has a system which: a) resides on one board, with a common interface to all functions, b) is easy to use (the user does not even need to know what "carrier phase ambiguity" means), and c) is robust, since

there is never a wrong decision made. It is at the cost of accuracy but that there are many users who only need 10-30 cm accuracy, and need a system which is robust and easy to use. It fills a niche which exists between pseudorange Positioning accuracy and fixed integer ambiguity carrier phase accuracy.

## SYSTEM DESCRIPTION

### Feature Summary

The following is a list of distinguishing properties that we believe are important in the RT20 positioning system.

- It derives accurate positions (<20 cm) and velocities (<2cm/sec)
- It is robust because it:
  - doesn't get wrong integers.
  - has RTCM link integrity.
  - has cycle slip detection in the tracking loops.
  - has a seamless transition from short to long baselines.
  - maintains ambiguities for all satellites, not just high ones.
- It has a high position rate (5 to 10 Hz) regardless of link rate.
- It has little accuracy degradation for correction delays of up to 3 seconds.
- It has improved on the fly estimation with kinematic specification through motion detection.

### Performance

This product functions as a normal 951R GPS card with an additional precise (20 cm) differential capability. The level of enhanced differential precision varies depending on a number of operational conditions, namely: DDOP, length in time of continuous tracking with at least 5 but preferably 6 strong satellites, delay in time between gathering the data at the monitor and the reception at the remote, and finally, the distance between the monitor and the remote station. Relative accuracy degrades significantly over long baselines if the reference station coordinates are incorrect, so good results presuppose that reference station errors are less than 15 metres. In addition, large multipath errors can bias the initial results significantly so the specifications quoted below are based on data collected in a reasonable, but not multipath free location.

Table 1 below summarizes the typical accuracy levels expected from the floating process under varying operational scenarios. Additional conditions that must be

fulfilled before these accuracy levels are achieved are that the DDOP must be less than 3 and there must be at least

6 satellites higher than 15 degrees elevation continuously tracked

Table 1: Performance Summary

Tracking Time (sec)	S/K*	Data Delay (sec)	Distance (km)	Accuracy (cm)
1 to 180	S	0	1	100 to 25
180 to 3000	S	0	1	25 to 5
3000 or more	S	0	1	5 or less
1 to 600	K	0	1	100 to 25
600 to 3000	K	0	1	25 to 5
3000 or more	K	0	1	5 or less
	S/K	0 to 2	1	+1 per sec
	S/K	2 to 7	1	+2 per sec
	S/K	7 to 20	1	+5 per sec
	S/K	20 to 60	1	+10 per sec
	S/K	60 or more	1	Single Point
	S/K	0	0 to 10	+0.5 per km
	S/K	0	10 to 20	+0.75 per km
	S/K	0	20 to 50	+1.0 per km

- Note: K = Kinematic (during initial ambiguity resolution)  
S = Static (during initial ambiguity resolution)

The performance characteristics of the time tagged positions are not significantly degraded during periods of increased dynamics, although the measurement latency will delay the position output. If the data link can provide at least one observation every 2 seconds, there will be no appreciable degradation in the accuracy of the intermediate positions that can be generated at a 10 Hz rate.

The velocity generated by this process is based on successive position differences, which in turn are generated from phase double differences. Therefore, velocity is an average generated over the delta time specified by the duty cycle of the RT20 filter. It has been observed that phase noise on antennas without choke ring ground planes will generate short-term baseline errors of 0.75 cm, and the monitor observation modeling error translates to an additional 1.0 cm/sec if the data link can provide an observation every 2 seconds. If the phase noise is uncorrelated, the resulting velocity error will be quite large when the maximum output rate is used. In fact, most of the phase noise is multipath induced, and shows a varying degree of correlation depending on the kinematic environment. When static data is processed in kinematic mode, the resulting velocity error is on the order of 2.0 cm/set, but this is probably an optimistic estimate because of the higher level of multipath correlation experienced by a stationary system.

### Robustness

We have found the real time double difference floating ambiguity system is much more stable than a single frequency fixed integer ambiguity system. All the points causing failure in a fixed integer system disappear. The wrong integers are never selected and the computed position variance better reflects the actual position errors. The system performance degrades gracefully as the length of the baseline increases. Unlike a fixed ambiguity system, this system will reliably generate better results the longer it is continuously running. Features such as motion detection make it possible to run the system with less operator intervention.

Part of the reason this is a robust system stems from various characteristics of the NovAtel GPSCard [1][2]. This is a low noise, multipath resistant receiver with strong tracking and reacquisition capabilities. Signals are often tracked through light obstructions, but if the signal is lost, it is quickly recovered when the visibility improves. In addition, the tracking software has a virtually fail-safe cycle slip detector. The reliability of the measurements makes a robust concept even more reliable.



lock indicator **pseudorange**, and phase for as many as 12 **satellites**. Thus the maximum **length of the type 59 message (without additional error correction)** is 744 bits. We suggest that the user **send** this message at a 2 second rate, although it could be slowed to 5 or 6 seconds if the user can use the matched **measurement position output (with a higher latency)** or accept the performance **degradation** (see Table 1).

### Initial Position

**The** initial controlling position is obtained from an RTCM **type 3** message transmitted **from the monitor**. The remote seed position is the best available local position generated from least squares pseudorange filter.

### Split in the data flow to M or G streams

Remote observations are matched with either measured and transmitted monitor observations encoded as an RTCM type 59 "N" message (the "M" stream) or monitor observations generated locally from a series of modeling Kalman filters (the "G" stream).

#### The M stream

The "M" stream is a data processor that acts upon time matched observations from the monitor and from the remote. The observations in the process are all observed, as opposed to a mixed set of observed and predicted observations that is used in the "G" stream. A secondary filter which accurately estimates delta position acts on data in this stream to generate an improved initial position and covariance estimate for the full state filter prior to its update. Only in **this** stream are both the position and ambiguity states estimated. This stream also maintains a bank of filters for estimation of monitor phase observations when these are unavailable.

Both remote and monitor observations are corrected for ionospheric and tropospheric delays **that are** estimated by position dependent atmospheric models. The tropospheric model assumes Standard meteorological conditions. During the matching process, the monitor observations are modified to be time synchronized to the **remote** observations.

#### The M Stream Filters

Double difference observations generated from the matched measured observation sets are used as inputs to the main Kalman filter. This filter estimates both position and ambiguities. The cold start position seed is an output of the concurrently running pseudorange least squares filter.

The **steady** state position **seed** is a position propagated from the last epoch with the application of a bridging **vector generated with a set of epoch to epoch matched** phase observations from the current epoch **and a best set** Of ambiguity estimates from the previous epoch The transition filter is identical to the main filter described below except that the ambiguity states are not included The error in the bridging **vector** is a result of noise on the observable and errors in the ambiguity estimate which translate into random and systematic position errors respectively The usual RMS **en-or** of the bridging vector is on the order **of** 0.006 metres so this **serves** the dual purpose of being a stabilizing transition function and as a reliable motion detector. If the magnitude of the transition vector is below threshold, it is not applied to the position state from the previous update and the process noise applied over the transition to the position state is eliminated.

Once tie position states and associated covariance have been propagated to the current epoch they are serially updated with both double difference phase and pseudorange observables according to the Kalman update equations, to generate current position and improved ambiguity state elements. The double difference observation covariance matrix is diagonalized prior to the update. The filter mechanism is described by the following set of equations.

The observables,  $\nabla\Delta\rho$  and  $\nabla\Delta\phi$  are double difference pseudorange and phase measurements described as follows:

$$\nabla\Delta\rho^i = \rho_r^i - \rho_r^0 - (\rho_m^i - \rho_m^0) \quad (1)$$

$$\nabla\Delta\phi^i = \phi_r^i - \phi_r^0 - (\phi_m^i - \phi_m^0) \quad (2)$$

The parameters of interest are the elements of the state vector given by:

$$\mathbf{x} = [x, y, z, \nabla\Delta N_1, \nabla\Delta N_2, \dots, \nabla\Delta N_n] \quad (3)$$

Where  $[x, y, z]$  is the ECEF vector between the monitor and remote stations and  $\nabla\Delta N_i$  is the double difference ambiguity between the stations and the  $i^{\text{th}}$  and reference satellite.

The observables and the state are related via the following linear relationships:

$$\nabla\Delta\phi^i = \mathbf{A}^i \mathbf{x} + \varepsilon_{\phi}^i \quad (4)$$

$$\nabla\Delta\rho^i = \mathbf{A}^i \mathbf{x} + \varepsilon_{\rho}^i \quad (5)$$

Where  $\mathbf{A}^i$  is the  $i^{\text{th}}$  row of the design matrix of differenced direction cosines to the  $i^{\text{th}}$  and reference satellite taken at the baseline reference position and given by:

$$\mathbf{A}^i = \begin{vmatrix} \frac{\partial \rho^i}{\partial x} - \frac{\partial \rho^0}{\partial x} & \frac{\partial \rho^i}{\partial y} - \frac{\partial \rho^0}{\partial y} & \frac{\partial \rho^i}{\partial z} - \frac{\partial \rho^0}{\partial z} & 0 & \dots & 1 & 0 \end{vmatrix} \quad (6)$$

for the phase relationship and

$$\mathbf{A}^i = \begin{vmatrix} \frac{\partial \rho^i}{\partial x} - \frac{\partial \rho^0}{\partial x} & \frac{\partial \rho^i}{\partial y} - \frac{\partial \rho^0}{\partial y} & \frac{\partial \rho^i}{\partial z} - \frac{\partial \rho^0}{\partial z} & 0 & \dots & 0 & 0 \end{vmatrix} \quad (7)$$

for the pseudorange equations.

### Statistical Representation of Position

The Kalman filter generating the state and its covariance assumes a white noise type error on its observations. In fact the observation errors show a high degree of correlation generated primarily by multipath but also ionospheric delays which become increasingly important as the station separation grows. The result of these conditions is that the covariance generated by the Kalman filter is too optimistic, especially after a long period of time. We have devised a rule based variance function dependent on baseline length and time from startup which generates statistics that more honestly reflect the errors in the system observed from the test data we have collected during the last several months.

### Monitor Observation Model

A set of Kalman filters is maintained to predict the monitor phase observations used in the G stream. Each filter models a single difference monitor observation rather than a nondifferenced observation so that any clock dynamics at the monitor are eliminated prior to the observations inclusion in its appropriate filter. Each

filter consists of three states maintaining the phase, phase rate and phase acceleration of its designated single difference monitor observation. In the differencing process, the same reference satellite is used as in the M streams ambiguity filter. If the reference changes, each filter is differenced appropriately to reflect the selection of the new reference.

The state related to the  $i^{\text{th}}$  satellite is described by the following vector:

$$\mathbf{x} = [\Delta\phi^i, \Delta\dot{\phi}^i, \Delta\ddot{\phi}^i] \quad (8)$$

where  $\Delta\phi^i = \phi^i - \phi^0$  and the process is implemented with a standard Kalman filter algorithm.

Tests have shown the RMS error of the propagated phase to be 0.028 cycles for a 2 second propagation and 0.386 cycles for a 6 second propagation.

### The G Stream

The G in this title stands for generated. In this stream, only the remote phase observations are measured. The matching monitor observations are based on single difference predictions. These are generated via the propagation of a series of Kalman filters, as described above. Time synchronized and atmospheric error removal is implicit because the observations on which the models are based have been corrected in the "M" stream. When an unmatched remote measurement appears, a monitor observation is generated via the propagation of the state described by equation (8). The resulting double difference observation is reduced by the current double difference ambiguity state, and then used in the position extrapolation filter to generate an extrapolated position. The error contributed by the extrapolation process is on the order of 1 or 2 centimetres under normal satellite geometry, provided the monitor messages are available every two seconds.

The relationship between the position state and phase observables is given by  $\nabla\Delta\phi - \nabla\Delta N = \mathbf{A}\mathbf{x} + \varepsilon$ , which is the same model as the transition filter.

Up to 10 positions per second can be generated with this filter.

### SYSTEM VERIFICATION

We have exercised various aspects of the system related to position and velocity accuracy under different operational conditions over the past six months. Particular areas of concern are the position latency and accuracy attained under different operational conditions.

## Latency

Two sources of latency which are of concern in this process are the delays associated with the data link and the delay between the measurement time and the time the generated position is output. The first stems from data link delays that are largely dependent on the transmission rate and integrity of the link. If a monitor message is transmitted at a lower rate, the accuracy of the monitor measurement filters at the remote will degrade, causing increased amounts of position error in the extrapolated positions. Tests have shown that link delays will produce single difference phase errors at the time of the update (i.e. error at the maximum propagation time) of 0.037 cycles (RMS) for a 2 second delay and 0.386 cycles (RMS) if the delay is 6 seconds. The 2 second delay will produce a maximum additional error of about 1 cm, while the 6 second delay produces a maximum error of about 10cm provided the DDOP is reasonable.

The time it takes to generate and format a position and send it to the COM port is on the order of 70msec. This was verified by triggering a counter with the GPS Card 1 PPS and stopping the count with the rising edge of the position output from the COM port.

## Accuracy

Position accuracy after different amounts of resolution time and under different dynamic conditions and over various baseline lengths is a primary concern in a positioning system. Areas that were investigated included the steady state precision of the system in static and kinematic environments. Conditions that degraded these results were studied and tests were devised to quantify the amount of this degradation. These included resolution time in static, kinematic and stop/go conditions.

**Table 2: Baseline Results**

Results Length (km)	Multi-path level	Reset Time (min)	Total Time (hr)	Horz Error Static (cm RMS)	Vert Error Static (cm RMS)	Horz Error Kinematic (cm RMS)	Vert Error Kinematic (cm RMS)
< .1	1	3	1.25	16.8	6.2	27.5	28.8
< .1	1	5	1.25	10.9	3.4	20.5	27.4
< .1	1	10	1.25	6.7	4.0	18.3	35.6
4.7	1	3	13	21.9	9.9	31.0	28.2
4.7	1	10	13	7.5	6.7	17.0	14.9
4.7	1	30	13	2.2	3.2	9.5	9.7
12	2	3	3.5	23.7	19.5	38.6	44.3
12	2	10	3.5	14.7	7.7	35.8	28.3
12	2	15	3.5	11.7	7.7	26.1	23.0
16	2	3	6	28.9	18.2	40.5	33.3

## Long Baseline Tests

We found it convenient to be able to collect and process large amounts of static data over baselines of varying lengths and over many days. With the cooperation of 3 number of our colleagues we were able to establish a network of rooftop collection sites from which large amounts of data were collected. The longest baseline in this network is 36 km and the shortest on the NovAtel roof, is 9 metres. The network of known points was established using previously established points as control and long term (many hours) RT20 solutions to extend it. The SemiKin [5] double difference program was used to verify enough RT20 computed points to be sure they contained no long term systematic errors. Redundancy was ensured through the use of closed loops and observations at more than one control point.

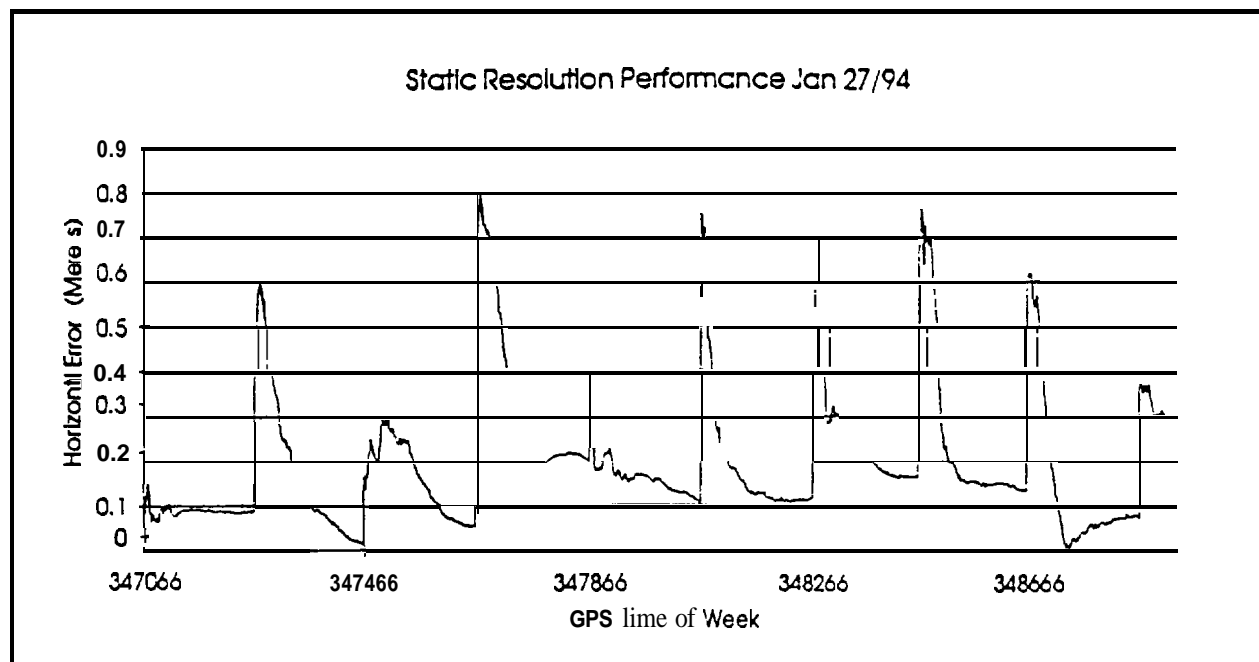
A series of data collection campaigns were undertaken during the spring and summer of 1994. Approximately 50 hours of data collected concurrently at 3 antennas or more were used to find and eliminate software errors in the floating ambiguity routines. Various performance aspects of the system were quantified. Among these were accuracy estimates after different lock times under static and kinematic conditions at varying baseline lengths. The results of these tests are summarized in the following tables. The first shows static data processed in kinematic mode. The sites had various multipath environments. Multipath levels are categorized below as 1, 2 or 3. Level 1 represents a level such as one would achieve with a choke ring at each antenna. Level 2 would represent one "typical" no-choke ring antenna and one choke ring. Level 3 represents two "typical" no-choke ring antennas.

16	2	10	6	13.6	7.1	30.5	18.8
16	2	30	6	6.3	5.1	13.9	11.0
20	2	3	4	23.2	24.6	39.6	46.3
20	2	10	4	12.2	9.9	15.7	21.5
20	2	15	4	8.9	4.7	14.7	17.2
36	3	3	19.5	82.1	55.4	76.4	82.6
36	3	10	19.5	39.4	27.3	84.0	46.6
36	3	30	19.5	15.6	10.0	57.0	29.1

As can be seen in Table 3, the lock-on performance is quite impressive when operating in static mode. An example of the performance of the system in static mode

during a period of resets timed every 200 seconds is seen in Figure 7,

**Figure 2:** Example Static Lock-on Performance



**Kinematic Tests**

A local control network was established near the NovAtel building in order to demonstrate the process to customers and to provide a framework for kinematic testing. Enough data was collected simultaneously at the control points on the road and at previously established points on the NovAtel roof and at the 25 Watt transmitter south of NovAtel so that the positions for these points could be reliably generated with SemiKin [5], the fixed ambiguity precise positioning package developed at the University of Calgary. As a check on the NovAtel RT20 algorithms, the same data was processed with a post mission version of the software and the largest discrepancy between these and the SemiKin results was 3cm.

The kinematic test used the markin feature of the GPSCard. The mark was triggered by a pulse from a

light sensitive sensor which recognizes returns from a series of reflective pieces of tape covering the local control points. The GPS antenna was attached to the top of the van so that it was aligned above the sensor mounted on the bottom of the van. The reflective strips were rectangular, dimensioned 5 cm along track and 8 cm cross track. The reflective sensor width covers a 1 cm diameter circle when it intercepts the ground. These uncertainties contribute some 9 cm to the expected horizontal uncertainty.

Systematic errors of 2.5 cm in north resulted from the centering of the reflective tape over the control. The sensor always picked the first reflective return, which was always 2.5cm early. Systematic errors of 10 cm in east resulted from a lateral tilt of some 10 degrees of the sensor mounted to the undercarriage of the van coupled with a lateral misalignment of the GPS antenna with the

sensor. The initial alignment of the sensor was a parking lot procedure while the test bed was a city street with the usual grade increase from curb to centerline. Both the north and east calibration errors were detected and measured during a calibration run during which the system had achieved near centimetre level accuracy. The direction dependent biases were measured from this and applied to all the data on subsequent tests. An additional height instrument error bias of 18 cm was also removed. The kinematic accuracy was verified during several independent campaigns. We wanted to find out how the

system would perform after three different resolution scenarios, namely static kinematic and a mixture of static and kinematic. The length of time each resolution process was allotted varied, and the length of each run lasted some 12 minutes after the resolution time. The number of "hits" generated during each run was subject to chance because of the size of the target and the placement of the sensor underneath the van. The results of the test are summarized in the following table.

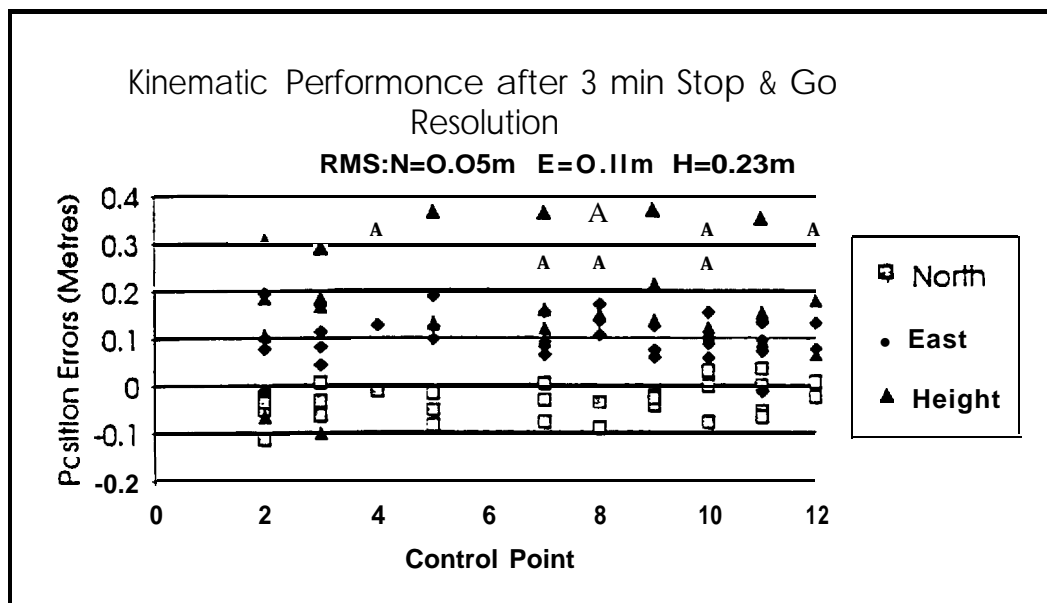
Table 3: Kinematic Test Summary

Res Scenario S/K/M	Res Time (min)	Me h	RMS h	Me v	RMS v
Static	3	0.12	0.13	0.30	0.31
	6	0.15	0.15	-0.16	0.16
	20	0.06	0.07	0.02	0.04
Kinematic	3	0.17	0.20	-0.47	0.48
	6	0.25	0.53	-0.55	0.56
	10	0.32	0.33	0.11	0.13
	20	0.58	0.62	0.04	0.28
Mix (50% S, 50%K)	3	0.11	0.12	0.20	0.23
	6	0.10	0.12	-0.53	0.60*
	10	0.22	0.23	-0.15	0.18
	20	0.04	0.23	-0.11	0.18

\* The anomalous behavior in the 6 minute stop and go resolution run is mitigated somewhat by the behavior of the height component error, which started the run 1 metre too low but slowly reduced in magnitude to 10 cm.

The stop and go resolution results were quite impressive. An example of these results is shown in Figure 3. The height component has a bias which reduces consistently during the period of data collection.

Figure 3: Position Errors after 3 Minutes Stop & Go



## CONCLUSIONS

The test results indicate that the following are true:

1a) The specifications shown in Table 1 have been achieved by this system in static and stop and go modes for short (<20km) baselines.

1b) The performance after a stop and go resolution is almost as good as the performance after a static resolution. This indicates that the motion detector is a valuable tool.

2) The static position accuracy was worse at 3 minutes than in the Table 1 specification for the long (36 km) baseline partly because neither antenna had a choke ring ground plane. This results in a higher multipath environment which degrades the results, especially at startup.

3) The true kinematic resolution produced lower than expected results. This test should be repeated to ensure that the number of satellites was not reduced through shading during the resolution process.

## ACKNOWLEDGEMENTS

We would like to thank Pat Fenton, Kip Fyfe, Jim Rooney, and Bryan Townsend, for the time they spent mounting antennas on their home rooftops and collecting data used for the long baseline tests. We also want to thank Doug Howard and Fraser Smith for their help in the kinematic test, and Wendy Corcoran for proofreading this paper.

We would also like to thank Dr. R. G. Brown for critiquing our Kalman Filter theory.

## REFERENCES

[1] Fenton, P., B. Falkenberg, T. Ford, Ng K., A.J. Van Dierendonck, **NovAtel's GPS Receiver - The High Performance OEM sensor of the Future, Proceedings of ION GPS '91**, Albuquerque, NM, Sept. 10-13. The Institute of Navigation, Washington, D.C., pp. 49-58.

[2] Van Dierendonck, A-J., P. Fenton and T. Ford (1992): **Theory and Performance of Narrow Correlator Spacing GPS Receiver**, Proceedings of the National technical Meeting U.S. Institute of Navigation, San Diego, Jan. 27-29, pp. 115-124.

[3] Brown RG. and Hwang P.Y.C, Introduction to Random Signals and Applied Kalman Filtering (2nd ed), New York John Wiley & Sons, Inc.,1992

141 Radio Technical Commission for Marine Services Paper 114-93/SC104-10, **RTCM Recommended Standards for Differential Navstar GPS Service, Washington 1993.**

[5] Cannon, ME.. High Accuracy GPS Semikinematic Positioning, Modelling and Results, Navigation. Journal of the Institute of Navigation, Vol. 37, No 1.